

perature protonation of **6** in CH_3OD led to regeneration of carbene complex **1**, which subsequently underwent acid-catalyzed isomerization to **2** at room temperature. Unlike other anions of electrophilic carbene complexes, which undergo C-alkylation, **6** is alkylated at rhenium.²⁵ For example, reaction of CH_3I with **6** produces *trans*- $\text{C}_5\text{H}_5(\text{CO})_2(\text{CH}_3)\text{Re}(\text{E})\text{-CH}=\text{CHCH}_2\text{C}(\text{CH}_3)_3$ (**7**).¹² The tendency of **6** to undergo alkylation at rhenium is related to the stability of $\text{C}_5\text{H}_5(\text{CO})_2\text{ReR}_2$ systems.²⁶

In summary, **1** is only the second example of a carbene complex that reacts with both nucleophiles and electrophiles at the carbene carbon atom. Derivatives of **1** are being synthesized to modulate the reactivity of the $\text{Re}=\text{C}$ multiple bond.

Acknowledgment. Support from the National Science Foundation is gratefully acknowledged. P.C.V. thanks BP America for a fellowship.

Supplementary Material Available: Full spectral characterization of compounds **1**–**7** (3 pages). Ordering information is given on any current masthead page.

(25) (a) Casey, C. P.; Anderson, R. L. *J. Organomet. Chem.* **1974**, *73*, C28. (b) Hegedus, L. S.; McGuire, M. A.; Schultze, L. M.; Yijun, C.; Anderson, O. P. *J. Am. Chem. Soc.* **1984**, *106*, 2680. (c) Bodner, G. S.; Smith, D. E.; Hatton, W. G.; Heah, P. C.; Georgion, S.; Rheingold, A. L.; Geib, S. J.; Hutchinson, J. P.; Gladysz, J. A. *J. Am. Chem. Soc.* **1987**, *109*, 7688.

(26) (a) Goldberg, K. I.; Bergman, R. G. *J. Am. Chem. Soc.* **1989**, *111*, 1285. (b) Hoyano, J. K.; Graham, W. A. G. *Organometallics* **1982**, *1*, 783.

Crystal and Molecular Structure of Dynemicin A: A Novel 1,5-Diyn-3-ene Antitumor Antibiotic

Masataka Konishi,* Hiroaki Ohkuma, Takashi Tsuno, and Toshikazu Oki

Bristol-Myers Research Institute, Tokyo Research Center
2-9-3, Shimo-Meguro, Meguro-Ku, Tokyo 153, Japan

Gregory D. VanDuyne and Jon Clardy*

Department of Chemistry, Baker Laboratory
Cornell University, Ithaca, New York 14853-1301

Received December 18, 1989

The antitumor antibiotics of the esperamicin¹ and calicheamicin² families have aroused considerable interest because of their exceptional potency,³ the structural novelty of their 1,5-diyne-3-ene core, and their intriguing mode of action.⁴ In this paper, we report

(1) (a) Golik, J.; Clardy, J.; Dubay, G.; Groenewold, G.; Kawaguchi, H.; Konishi, M.; Krishnan, B.; Ohkuma, H.; Saitoh, K.; Doyle, T. W. *J. Am. Chem. Soc.* **1987**, *109*, 3461–3462. (b) Golik, J.; Dubay, G.; Groenewold, G.; Kawaguchi, H.; Konishi, M.; Krishnan, B.; Ohkuma, H.; Saitoh, K.; Doyle, T. W. *J. Am. Chem. Soc.* **1987**, *109*, 3462–3464.

(2) (a) Lee, M. D.; Dunne, T. S.; Siegel, M. M.; Chang, C. C.; Morton, G. O.; Borders, D. B. *J. Am. Chem. Soc.* **1987**, *109*, 3464–3466. (b) Lee, M. D.; Dunne, T. S.; Chang, C. C.; Ellestad, G. A.; Siegel, M. M.; Morton, G. O.; McGahren, W. J.; Borders, D. B. *J. Am. Chem. Soc.* **1987**, *109*, 3466–3468.

(3) Maiese, W. M.; Lechevalier, M. P.; Lechevalier, H. A.; Korshalla, J.; Kuck, N.; Fantini, A.; Wilder, M. J.; Thomas, J.; Greenstein, M. *J. Antibiot.* **1989**, *42*, 558–563.

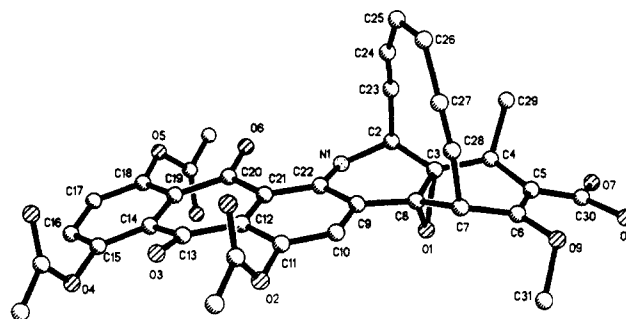
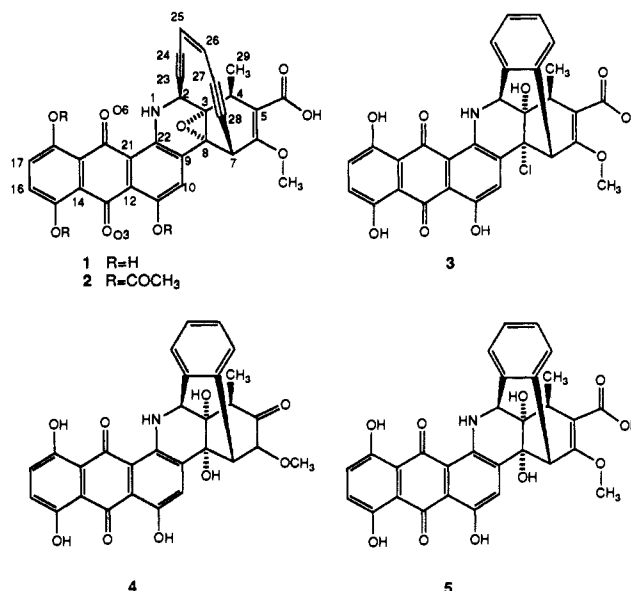


Figure 1. A computer-generated perspective drawing of the final X-ray model of dynemicin A triacetate (**2**). Hydrogens are omitted for clarity, and no absolute configuration is implied.

the structure of another 1,5-diyne-3-ene antibiotic: dynemicin A (**1**) from *Micromonospora chersina*.⁵ Dynemicin A (**1**) has potent inhibitory activity against a wide range of bacteria and tumor cell lines, a structurally novel fusion of an anthraquinone with a tetracyclo 1,5-diyne-3-ene, and a putative mode of action similar to the esperamicins and calicheamicins.



Dynemicin A was isolated⁵ from the ethyl acetate extract of *M. chersina* as a lipophilic violet solid: HRMS m/z 538.1132 ($M + H$); $\text{C}_{30}\text{H}_{19}\text{NO}_9 + \text{H}$ requires 538.1138; mp 208–210 °C dec; $[\alpha]_D^{20} +270^\circ$ (c 0.01, DMF); IR (KBr) 3420, 3350, 2930, 1660, 1630, 1587, 1480, 1385, 1300, 1280, 1180, and 785 cm^{-1} ; UV (MeOH) λ_{max} 239 (ϵ 24 900), 282 (sh), 569 (10 800), and 599 nm (10 100). The UV spectrum and the absorption shifts observed in weakly acid and alkaline solution⁶ suggested a 1,4,5,8-tetrahydroanthraquinone chromophore. Poor solubility hampered spectral characterization of **1**,⁷ but conversion to its triacetate **2** (acetic anhydride–pyridine, 25 °C) provided a more tractable material. The ^{13}C NMR spectrum of **2** revealed a 1,2,4,5,8-pentasubstituted anthraquinone (δ_{C} 146.9, s, C18; 130.6, d, C17; 131.0, d, C16; 146.4, s, C15; 125.9, s, C14; 180.6, s, C13;

(4) (a) Zein, N.; Sinha, A. M.; McGahren, W. J.; Ellestad, G. A. *Science* **1988**, *240*, 1198–1201. (b) Long, B. H.; Golik, J.; Foreza, S.; Ward, B.; Rehuss, R.; Dabrowiak, J. C.; Catino, J. J.; Musial, S. T.; Brookshire, K. W.; Doyle, T. W. *Proc. Natl. Acad. Sci. U.S.A.* **1989**, *86*, 2–6.

(5) Konishi, M.; Ohkuma, H.; Matsumoto, K.; Tsuno, T.; Kamei, H.; Miyaki, T.; Oki, T.; Kawaguchi, H.; VanDuyne, G. D.; Clardy, J. *J. Antibiot.* **1989**, *42*, 1449–1452.

(6) UV: λ_{max} in 0.01 N HCl–MeOH 240 (ϵ 26 300), 284 (sh), 572 (10 100), and 596 nm (10 300); in 0.01 N NaOH–MeOH 247 (ϵ 22 600), 278 (5400), 598 (11 500), and 644 nm (11 300). See: Oki, T.; Yoshimoto, A.; Matsuzawa, Y.; Takeuchi, T.; Umezawa, H. *J. Antibiot.* **1980**, *33*, 1331–1340.

(7) ^1H NMR of **1** (400 MHz in $\text{DMSO}-d_6$): δ 1.30 (3 H, d, $J = 7.3$), 3.57 (1 H, q, $J = 7.3$), 3.82 (3 H, s), 4.89 (1 H, s), 5.08 (1 H, d, $J = 4.3$), 6.06 and 6.09 (AB quartet, $J = 9.8$), 7.33 (1 H, d, $J = 8.9$), 7.38 (1 H, $J = 8.9$), 8.03 (1 H, s), 9.86 (1 H, d, $J = 4.3$), 12.15 (1 H, br s), 12.30 (1 H, v br s), 12.70 (1 H, br s), 13.10 (1 H, br s).

124.5, s, C12; 139.5, s, C11; 130.0, d, C10; 130.1, s, C9; 143.8, s, C22; 114.7, s, C21; 182.7, s, C20; 126.1, s, C19) as well as a 1,5-diyne-3-ene system (δ_C 97.3, s, C23; 89.6, s, C24; 124.4, d, C25; 124.0, d, C26; 88.8, s, C27; 99.4, s, C28).⁸ Triacetate **2** was further characterized by single-crystal X-ray diffraction.

The dark orange crystals of **2** belonged to the monoclinic space group $P2_1$ with $a = 9.238$ (4) Å, $b = 13.047$ (5) Å, $c = 28.254$ (9) Å, and $\beta = 98.62$ (3)°. The crystal density required that two molecules of triacetyldynemicin A (**2**) form the asymmetric unit ($Z = 4$). All unique diffraction maxima with $2\theta \leq 100^\circ$ were collected by using variable-speed Wyckoff scans and graphite-monochromated Cu $K\alpha$ radiation. Of the 3403 independent reflections surveyed in this manner, 2684 (79%) were judged observed ($|F_o| \geq 4.0\sigma(F_o)$) after correction for Lorentz, polarization, and background effects. A phasing model was found with some difficulty, and successive electron density syntheses finally revealed the entire nonhydrogen atom structure. Some hydrogen atoms were located in subsequent difference electron density syntheses, but the majority were included at appropriate locations. Blocked full-matrix least-squares refinements with anisotropic heavy atoms and fixed isotropic hydrogens have converged to a standard crystallographic residual of 8.4% for the observed data.

A computer-generated perspective drawing of the final X-ray model of triacetyldynemicin A (**2**) is given in Figure 1. The X-ray experiment defined only the relative, not the absolute configuration, and the enantiomer shown was selected arbitrarily. Attempts to prepare heavy-atom derivatives of dynemicin in order to determine the absolute configuration via anomalous dispersion techniques have not yet succeeded. There are two independent molecules in the asymmetric unit, and while they have the same overall structure, their conformations are distinctly different. In the molecule shown, the anthraquinone ring is bowed so that O3 and O6 are pushed up, on the same side of the molecule as the 1,5-diyne-3-ene moiety. The anthraquinone fragment is bowed so that there is a shallow concave surface on the bottom of the molecule, on the side away from the 1,5-diyne-3-ene moiety. In the other independent molecule, the bowing of the anthraquinone occurs in the opposite sense; O3 and O6 are on the bottom, as is the convex face of the anthraquinone. The bowing may be described more quantitatively by considering the dihedral angles between the right- and left-hand aromatic rings of the anthraquinone. In one conformation, it is 12°, and in the other, 17° in the opposite sense.

This X-ray structure of triacetyldynemicin A represents the first time that a naturally occurring 1,5-diyne-3-ene has been characterized by X-ray diffraction, but the geometry is similar to that observed in earlier model studies.⁹ The alkynes are bent substantially from linearity while the alkene is essentially normal. The angles for the two different conformations are as follows: C24, 161.9° and 169.6°; C23, 165.5° and 164.0°; C27, 160.2° and 172.5°; and C28, 168.3° and 162.1°. Since the estimated standard

deviation in these measurements is $\pm 2^\circ$, it is not clear that the two different crystal conformations observed for the anthraquinone portion have structural consequences for the 1,5-diyne-3-ene fragment. The methyl group at C4, C29H₃, makes a close approach to the 1,5-diyne-3-ene bridge with a closest distance of 2.93 (3) Å and 3.07 (3) Å to C23. Carbons 23 and 28 are separated by 3.54 (3) Å.⁹

With the structures of **1** and **2** fully defined, the structures of some of the minor dynemicins—L (**3**, C₃₀H₂₂NO₉Cl), M (**4**, C₂₉H₂₃NO₉), and N (**5**, C₃₀H₂₃NO₁₀)—could be established spectroscopically.¹⁰ The ¹³C NMR spectra of **3–5** exhibited signals for the anthraquinone moiety essentially identical with those of **1**. The spectrum of **3** lacked both the characteristic four singlet carbon resonances of the conjugated acetylene (δ_C 88.8–99.4) and the two doublet protons of the alkene (δ_H 6.06 and 6.09) observed in **1** and **2**. The presence of four new sp² carbon signals around δ_C 126.2–135.6 and signals for four contiguous aromatic protons (δ_H 7.10–7.60) strongly argued that the 1,5-diyne-3-ene had aromatized. The epoxide had also disappeared and been replaced by a chlorine at C8 and a hydroxyl at C3 as indicated by homo- and heteronuclear shift correlation spectroscopies. Thus dynemicin L is **3**. Dynemicin N (**5**) was very similar to **3**, but its molecular formula and spectroscopic data indicated that the chlorine in **3** was replaced by a hydroxyl in **5**. The ¹³C NMR spectrum of dynemicin M (**4**) was generally similar to the spectra of **3** and **5**, but displayed a new ketone (δ_C 204.8) and a new sp³ carbon (δ_C 82.7, d) at the expense of the carboxyl (δ_C 167) and the two sp² carbons (δ_C 113–114 and 153–159). Structure **4** is fully consistent with the spectral data for dynemicin M. Further support for structures **3** and **5** was provided by allowing **1** to stand in an acidic solution at room temperature and watching its rapid conversion to **3** followed by the gradual appearance of **5**. This decomposition experiment also indicates that the epoxide ring can open easily to relax the strain of the 1,5-diyne-3-ene embedded in the 10-membered ring and bring C23 and C28 close enough to cyclize to an aromatic ring. This mechanism, with the replacement of the epoxide by a bridgehead double bond, is the proposed mode of action of the esperamicin/calicheamicin class of antibiotics.⁴ The epoxide of dynemicin A (**1**) is also reminiscent of the epoxide in the neocarzinostatin chromophore, but in the neocarzinostatin case, opening of the epoxide yields an isolable chlorohydrin.¹¹ The decomposition experiment also raises the possibility that dynemicins L (**3**), N (**5**), and possibly M (**4**) are artifacts of the isolation.

Dynemicin A (**1**) and triacetyldynemicin A (**2**) display strong activity against Gram-positive bacteria with **2** being 2–8 times more active against a range of test organisms. Both compounds show marked cytotoxic activity against B16 melanoma, Moser human carbinoma, HCT-116 human carcinoma, and the normal and vincristine-resistant P388 leukemia cells with IC₅₀ values of 0.004–0.005 µg/mL. In vivo tests, both **1** and **2** produced significant prolongation of life span in P388 leukemia and B16 melanoma inoculated mice. Unlike the esperamicin antibiotics, **1** exhibits significant in vivo antibacterial activity and low toxicity. Dynemicins L, M, and N do not show significant levels of activity.

Acknowledgment. We are particularly grateful to Professor M. Ohashi and Dr. H. Kawaguchi, T. Naito, and T. W. Doyle for their help and stimulating discussions on this work. This work was partially supported by NIH Grant CA24487 to J.C.

Supplementary Material Available: ¹H NMR spectral data for triacetyldynemicin A (**2**), physicochemical properties and spectral data for dynemicins L (**3**), M (**5**), and N (**4**), and X-ray crystallographic data for triacetyldynemicin A (**2**) (21 pages). Ordering information is given on any current masthead page.

(8) Triacetyldynemicin A (**2**): orange rods from aqueous MeOH; mp 228–231 °C dec; $[\alpha]_D^{25} +1300$ (c 0.05, MeOH) λ_{max} 224 (ϵ 40 100), 313 (6700), and 482 nm (8100); ¹H NMR (DMSO-*d*₆, 400 MHz) δ 1.25 (3 H, d, $J = 7.3$, 29-H), 2.33, 2.36, and 2.44 (3 H each, s, COCH₃), 3.55 (1 H, q, $J = 7.3$, 4-H), 3.79 (3 H, s, 31-H), 4.78 (1 H, s, 7-H), 5.04 (1 H, d, $J = 3.8$, 2-H), 6.05 (1 H, dd, $J = 9.8$ and 1.3, 25-H), 6.07 (1 H, dd, $J = 9.8$ and 1.3 Hz, 26-H), 7.62 (2 H, s, 16-H and 17-H), 8.03 (1 H, s, 10-H), 9.41 (1 H, d, $J = 3.8$, 1-NH), 12.37 (1 H, br, 30-OH); ¹³C NMR (DMSO-*d*₆, 100 MHz) δ 43.8 (d, C2), 71.3 (s, C3), 35.6 (d, C4), 114.8 (s, C5), 153.2 (s, C6), 31.4 (d, C7), 63.0 (s, C8), 130.1* (s, C9), 130.0* (d, C10), 139.5 (s, C11), 124.5 (s, C12), 80.6 (s, C13), 125.9 (s, C14), 146.4 (s, C15), 131.0 (d, C16), 130.6 (d, C17), 146.9 (s, C18), 126.1 (s, C19), 182.7 (s, C20), 114.7 (s, C21), 143.8 (s, C22), 97.3 (s, C23), 89.6 (s, C24), 124.4 (d, C25), 124.0 (d, C26), 88.8 (s, C27), 99.4 (s, C28), 18.5 (q, C29), 167.3 (s, C30), 57.7 (s, C31), 20.6 × 2 and 20.9 (COCH₃), 168.9 and 169.1 × 2 (COCH₃). Assignments with an asterisk (*) may be interchanged. Anal. Calcd for C₃₀H₂₅NO₁₂·H₂O: C, 63.43; H, 3.99; N, 2.06. Found: C, 63.20; H, 3.75; N, 2.16.

(9) (a) Magnus, P.; Lewis, R. T.; Huffman, J. C. *J. Am. Chem. Soc.* **1988**, *110*, 6921–6923. (b) Schoenen, F. J.; Porco, J. A.; Schreiber, S. L.; Van-Duynne, G. D.; Clardy, J. *Tetrahedron Lett.* **1989**, *30*, 3765–3768. (c) Danishefsky, S. J.; Mantlo, N. B.; Yamashita, D. S.; Schulte, G. *J. Am. Chem. Soc.* **1988**, *110*, 6890–6891. (d) Nicolaou, K. C.; Zuccarello, G.; Ogawa, Y.; Schweiger, E. J.; Kumazawa, T. *J. Am. Chem. Soc.* **1988**, *110*, 4866–4868. (e) Snyder, J. P. *J. Am. Chem. Soc.* **1989**, *111*, 7630–7632 and references therein for a theoretical analysis.

(10) **3**: blue powder; mp 222–225 °C; $[\alpha]_D^{25} -820^\circ$ (c 0.10, MeOH); λ_{max} 241 (ϵ 48 100), 454 (2400), 594 (18 000), 639 nm (17 900). **4**: blue powder; mp 238–240 °C; $[\alpha]_D^{25} -2460^\circ$ (c 0.01, MeOH); λ_{max} 241 (ϵ 41 700), 453 (1500), 589 (17 000), 633 nm (17 200). **5**: blue powder; mp 253–256 °C; $[\alpha]_D^{25} -200^\circ$ (c, 0.01, MeOH); λ_{max} 241 (53 100), 452 (4300), 592 (24 500), 639 nm (25 200).

(11) Edo, K.; Mizugaki, M.; Koide, Y.; Seto, H.; Furihata, K.; Otake, N.; Ishida, N. *Tetrahedron Lett.* **1985**, *26*, 331–335.